

Fundamental parameters of isolated galaxy triplets in the local Universe: Statistical study

Amira A. Tawfeek,^{1,2*} Gamal B. Ali,¹ Ali Takey,¹ Zainab Awad,² and Z. M. Hayman²

¹National Research Institute of Astronomy and Geophysics (NRIAG), 11421 Helwan, Cairo, Egypt

²Astronomy, Space Science and Meteorology Department, Faculty of Science, Cairo University, 12613 Giza, Egypt

Accepted XXX. Received YYY; in original form ZZZ

ABSTRACT

Understanding the dynamics of galaxy triplet systems is one of the significant ways of obtaining insight into the dynamics of large galaxy clusters. Toward that aim, we present a detailed study of all isolated triplet systems (total of 315) taken from the “SDSS-based catalogue of Isolated Triplets” (SIT). In addition, we compared our results with those obtained for a sample of triplets from the Local Supercluster (LS), SDSS-triplets, Tully’s catalogue, Wide (W) and Compact (K)-triplets. In addition, we performed the correlation between the dynamical parameters and the Large Scale Structure (LSS). Interestingly, we found that there is no correlation between both the mean projected separation for the triplet systems and the LSS and its dynamical parameters. Furthermore, we found that only 3% of these systems can be considered as compact since the mean harmonic separation (r_h) is more than 0.4 Mpc for 97% of the population. Thus we may conclude that, mergers might not have played a dominant role in their evolution.

Key words: galaxies: fundamental parameters – galaxies: groups: general – galaxies: statistics

1 INTRODUCTION

Galaxies are no longer considered as island universes. They aggregate to form pairs, triplets, groups (not more than 50 galaxies) or clusters (up to 300 galaxies) (Bahcall 1996). Recently, it was found that 54% of the galaxies in the local Universe (with redshifts smaller than 0.1) aggregate into galaxy groups and clusters, while 20% are located in collapsing regions around these groups and clusters. The rest (26%) are field galaxies (Blanton et al. 2003, and references therein).

Galaxy triplets were first thought to be formed as close binaries then a remote galaxy is attracted later as a third body (Valtonen & Mikkola 1991; Chernin et al. 1994). This scenario is no longer held since Kiseleva (2000) found that triplets are groups of three member galaxies immersed in a dark matter halo without an observed formation of close binaries. Therefore, triplets are a special type of galaxy groups with the smallest number of members (Duplancic et al. 2015). Galaxy triplets have nearly the same complexity of larger groups; statistics, dynamics, and evolutionary properties. They are characterised by their proximity and low relative velocities which make them ideal for studying

galaxy interactions and merging scenarios (Duplancic et al. 2013).

The first triplet catalogue, which included 84 Northern isolated galaxy triplets, was compiled by Karachentseva et al. (1979). They used visual inspection of the Palomar Sky Survey prints to observe these systems and study some of their observational properties. According to their procedure, triplet systems were constructed with members of apparent magnitudes brighter than 15.7 mag and angular diameter between 0.5 and 2 arcmin. Thus, a given triplet system which satisfied this criterion, is said to be isolated if the distance to its nearest neighbour is 3 times larger than the average distance between its galaxy members. This criteria yielded to select triplet member galaxies regardless of their radial velocity (v), and hence a system may be isolated only in projection. For these reasons, Karachentsev & Karachentseva (1981); Karachentsev et al. (1988) conducted spectroscopic observations and numerical studies on this catalogue and found that only 64% of the observed systems can be considered physical triplets with velocity differences $\Delta v < 500 \text{ km s}^{-1}$.

Although triplets were thought to represent a collection of unrelated field galaxies rather than physical structures, recent analysis by Hernández-Toledo et al. (2011) showed that these galaxies have signatures of physical interactions

* E-mail: amira_nriag@yahoo.com

which infer that most of them are indeed real physical structures. These interactions have a strong effect on the fundamental properties of their galaxies such as star formation rate, nuclear activity, and morphology (O’Mill et al. 2012). Moreover, it is well known that interactions are common in triplets and compact systems in which they may end up into a single system (Duplancic et al. 2013). Hence, studying these systems is crucial to understand their origin, evolution, intrinsic structure and how the surrounding environment affects their morphological, physical, and dynamical characteristics.

The key aim of this work is to conduct a statistical study on the 315 triplet systems from “SDSS-based catalogue of Isolated Triplets”(SIT) (Argudo-Fernández et al. 2015) to estimate their basic parameters; namely, radial velocities (v), distances (D), angular separations (θ), projected separations (r_p), mean harmonic separation (r_h), velocity dispersion (σ), virial masses (M_{vir}/M_\odot), luminosity (L_r), absolute magnitudes (M_r), and mass-to-light ratios (M_{vir}/L_r). Accordingly, we will distinguish between compact (k) and wide (w) triplets in our sample according to their mean harmonic separation (r_h). Then, we will compare our results with another documented triplets sample. Finally, we will investigate the correlations between the dynamical parameters of the studied triplet systems and the Large Scale Structure (LSS).

This paper is organised as follows; in § 2 we introduce our sample and the calculated basic parameters for each system and its three members. The results of the statistical study and the correlations between the triplet parameters are presented and discussed in § 3 while the main conclusions and remarks are given in § 4.

2 SAMPLE DESCRIPTION AND THEIR FUNDAMENTAL PARAMETERS

In this section we briefly describe the chosen sample and discuss in some details the calculations of some fundamental parameters of each system and its galaxy members.

2.1 The chosen sample

We conduct a statistical study on 315 galaxy triplet systems taken from the SIT catalogue by Argudo-Fernández et al. (2015). This catalogue is based on the Sloan Digital Sky Survey- Tenth Data Release (SDSS-DR10 Ahn et al. 2014). Triplet systems (in this selected catalogue) are restricted to have members with spectroscopic information, r-band model magnitudes (m_r) in the range $14.5 \leq m_r \leq 17.7$ over a redshift (z) range $0.006 \leq z \leq 0.080$. Argudo-Fernández et al. (2015) based their isolation criterion on galaxies with no neighbours within radial velocity difference $\Delta v \leq 500 \text{ km s}^{-1}$ and all galaxies are found within 1 Mpc radius ($d \leq 1 \text{ Mpc}$). In addition, they performed a star-galaxy separation in order to prevent classifying a star as a galaxy and removed multiple identifications of the same galaxy. Hence, they based their isolation criteria mainly on both the velocity difference (Δv) and the projected distance space. Following this criteria they compiled a catalogue of 315 isolated triplet systems. SDSS coloured images of some triplet systems of these catalogue are illustrated in appendix A. In these systems, galaxies are considered to be physically

bounded to the primary galaxy (chosen to be the brightest one in the member), if $\Delta v \leq 160 \text{ km s}^{-1}$, and the projected separation (r_p) is smaller than 450 kpc.

We choose this catalogue in our study because (i) it compiles a large sample of triplet galaxies (315 systems), (ii) triplets are isolated with no neighbours for at least 1 Mpc radius and hence there is no interaction with the surrounding environment, (iii) isolated triplets have been homogeneously selected, with a hierarchical structure, using an automated method, and (iv) all triplet galaxies have spectroscopic information and their galaxy parameters (RA, DEC, z) are available.

The observational parameters (apparent magnitude (m_r) in the r-band, k-correction, the luminosity distance (D_L), the photometric and spectroscopic redshifts) were extracted from CasJobs tool in SDSS DR12 (Alam et al. 2015a). These parameters are helpful in estimating other basic parameters such as; the absolute magnitude (M_r) in r-band, and the radial velocity (v). The SDSS-DR12 is the final data release of the SDSS-III which contains observations up to July 2014. It covers the complete dataset of the BOSS, APOGEE, and the stellar radial velocity measurements from MARVELS surveys. SDSS-DR12 includes all information in DR11 and previous releases of SDSS (Alam et al. 2015b). Throughout this study we compute the statistical parameters based on the spectroscopic redshift which is more accurate than the photometric one. Furthermore, spectroscopic redshift does not have the neighbouring effect that influences the photometric measurements (Patton et al. 2011; Shen et al. 2016)

2.2 Galaxy triplets: fundamental parameters

In the following context we describe briefly the calculations of both the dynamical (σ , r_h , M_{vir}/M_\odot , and M_{vir}/L_r) and physical parameters (v , θ , r_p , M_r , L_r) of the triplet systems and their members, respectively, and show how they are linked together. Each triplet system is characterised by its σ , r_h , M_{vir}/M_\odot , and M_{vir}/L_r while for each member galaxy in the system we calculate the rest of the basic parameters; see Tables 1 and 2. The adopted constants in the calculations throughout this work are: Hubble constant ($H_0 = 70 \text{ km s}^{-1} \text{ Mpc}^{-1}$), speed of light ($c = 2.99792 \times 10^5 \text{ km s}^{-1}$), gravitational constant ($G = 6.674 \times 10^{-11} \text{ m}^3 \text{ kg}^{-1} \text{ s}^{-2}$), the solar absolute magnitude and colour are taken from SDSS where ($M_{\odot,g}$ (in g-band) = 5.12 ± 0.2), and ($M_{\odot,g-r}$) = 0.44 ± 0.02). The solar absolute magnitude in r-band $M_{\odot,r}$ can be computed by subtracting $M_{\odot,g}$ in g-band from $M_{\odot,g-r}$; thus $M_{\odot,r} = 4.68$, and solar mass ($M_\odot = 1.9891 \times 10^{30} \text{ kg}$). Details on the calculations of $M_{\odot,r}$ are given in the website of SDSS¹, and (Blanton et al. 2003; Bilir et al. 2005; Rodgers et al. 2006).

Triplet as a unit dynamical system and their members are characterised by the following parameters:

- (i) Physical parameters
 - **Angular separation (θ_{ik}) in arcmin**

¹ www.sdss.org/dr14/algorithms/ugrizVegaSun/

Angular separation can be calculated by two methods: one is applying Equation 1 as taken from Smart (1965)

$$\theta_{ik} = \{ \cos^{-1} [\sin(\delta_{ik}) \sin(\delta_{ik}) + \cos(\delta_{ik}) \cos(\delta_{ik}) * \cos((\alpha_{ik}) - (\alpha_{ik}))] \}, \quad (1)$$

where $i, k=1, 2, 3; i \neq k$, δ is the declination and α is the right ascension of the galaxy. The other method is using the python module “*astCoords.calcAngSepDeg*” in *AstLib*². We obtained the same results using both methods.

• Projected separation (r_p) in Mpc

Projected separation is defined as the minimum separation between two celestial objects determined by the product of the distance ($D=v/H_0$) and the angular separation (θ) between them (Chernin et al. 2000; Ali 2001; Vavilova et al. 2005; ?). Hence, we can estimate the projected separation between each two galaxies in the triplet systems by using the generalised equation

$$r_p = 2 < v > H_0^{-1} \sin(\theta_{ik}/2), \quad (2)$$

where v is the radial velocity defined as the product of speed of light (c) and the redshift (z) in $km s^{-1}$ ($v = cz$) (Dekel & Ostriker 1999; Schneider 2006), θ_{ik} is the angular separation between the members of each triplet system, $i, k=1, 2, 3; i \neq k$.

(ii) Dynamical parameters

• Velocity dispersion (σ) in $km s^{-1}$

After estimating the radial velocity (v) of the three galaxies in a triplet system, we can compute the system velocity dispersion (σ) following the expression

$$\sigma = [< (v)^2 > - (< v >)^2]^{\frac{1}{2}}, \quad (3)$$

where $< >$ denotes the average overall the members of the system (Chernin et al. 2000; Schneider 2006; Duplancic et al. 2015).

• Mean harmonic separation (r_h) in Mpc

The mean harmonic separation (r_h) is a remarkable parameter suitable for cosmological investigations since it is not specified for a certain type of groups or clusters. It represents the angular size of the core of a galaxy group or cluster. It depends on the position of the brightest galaxy in the group or cluster, and thus it is important in studying very distant clusters where only the brightest galaxies could be visible. Since, this parameter represents the core size of the group or cluster, it is strongly related to their gravitational radius and therefore has a statistical power (Hickson 1977a,b). Harmonic separation is based mainly on the projected separation (r_p , see above) between members of a triplet system. It indicates whether the members are close to each other (i.e. compact) or far from each other (i.e. loose). Therefore, determination of r_h is important to categorise the systems into wide (w) and compact (k) following Chernin et al. (2000) as

$$r_h(Mpc) = \begin{cases} < 0.04 & \text{compact system (k)} \\ > 0.04 & \text{wide system (w)} \end{cases}$$

The general formula of the mean harmonic separation (r_h) is expressed in terms of N , the number of galaxies in a given group or cluster, as

$$r_h = [(2/N(N-1)) \Sigma r_{pik}^{-1}]^{-1}, \quad (4)$$

where $i, k=1, 2, \dots, N; i \neq k$ (Hickson 1977a)

In the case of triplet galaxies, $N=3$, Equation 4 will be re-written as

$$r_h = [(1/3) \Sigma r_{pik}^{-1}]^{-1}, \quad (5)$$

where $i, k=1, 2, 3; i \neq k$ (Chernin et al. 2000; Vavilova et al. 2005; Feng et al. 2016).

• Virial Mass (M_{vir}/M_\odot)

For a system of N members occupied in a circle of minimum radius R , that contains the centres of these members, the virial mass is given by

$$M_{vir} = 3\pi N(N-1)^{-1} G^{-1} \sigma^2 R, \quad (6)$$

For triplets, $N=3$, we have

$$M_{vir} = (9\pi/2G) R \sigma^2, \quad (7)$$

where G is the gravitational constant, R can be considered to be the mean harmonic separation r_h in meters, and σ is the velocity dispersion in $m s^{-1}$ (Chernin et al. 2000; Vavilova et al. 2005; Liljeblad 2012; Duplancic et al. 2015).

• Mass-to-Light ratio (M_{vir}/L_r)

To compute the mass-to-light ratio of a system of galaxies, we first have to calculate the luminosity of each galaxy (L_r , in r-band) using the following equation

$$L_r = dex[0.4(M_{\odot,r} - M_r)], \quad (8)$$

where $M_{\odot,r}$ and M_r are the solar and galactic absolute magnitudes in the r-band, respectively (Binney & Tremaine 1987; Ali 2001; Schneider 2006).

The absolute magnitude of a galaxy in the r-band is given by

$$M_r = m_r - 5(\log(D_L - 1)) - k_{corr}, \quad (9)$$

where m_r is the apparent magnitude in r-band corrected from reddening, D_L is the luminosity distance in pc, and k_{corr} is the k-correction in the r-band. These parameters are obtained from the SDSS database.

Therefore, the mass-to-light ratio (M_{vir}/L_r) is

$$M_{vir}/L_r = M_{vir}/dex[0.4(M_{\odot,r} - M_r)], \quad (10)$$

where in Equation 10, L_r is the total luminosity of the three members in each system ($L_r = \sum_{n=1}^3 L_{r,n}$).

² <http://astlib.sourceforge.net/docs/astLib/astLib.astCoords-module.html>

Tables 1 and 2 summarise our calculations of both the physical and dynamical parameters of the triplet systems and their members for the studied catalogue SIT (Argudo-Fernández et al. 2015). In Table 2, the maximum value of the mass-to-light ratio is computed for 313 triplet systems only as we excluded two systems (SIT 99 and SIT 168) due to their very large ratios (567 and 810, respectively). Each of these two systems compose of very faint galaxies (G1, G2, and G3), especially the third galaxy (G3), which make their total luminosity very small, and hence, the mass-to-light ratio becomes greater than usual. On the other hand, the other dynamical parameters (σ , M_{vir}) for these systems fall in the normal range. The computed dynamical parameters of the 315 studied triplet systems from SIT are listed in Table A1 (see Appendix A).

3 RESULTS AND DISCUSSION

Statistical studies of galaxy triplet systems are crucial in understanding the main properties and the evolution of galaxies in groups. Analysis of such poor populated groups (3 members) is an important step to study more populated groups. In this section, we present the distribution of the basic parameters of triplet systems that control their properties. Then, we demonstrate the satellite to central galaxy ratios of both absolute magnitude (M_r) and luminosity (L_r), in the r-band. In addition, the correlation between the dynamical parameters of the studied triplets and their mean projected separation (\bar{r}_p) is determined by calculating their correlation coefficients (f_{xy}). Finally, we illustrate the correlation between triplets' dynamical parameters and the surrounding Large-Scale Structure (LSS).

3.1 Distributions of galaxy triplets parameters

Fig. 1 represents the distribution of the calculated basic parameters of the studied 315 triplet systems. Fig. 1a demonstrates the distribution of the projected separation (r_p) showing a multi-modal distribution with a mean value 0.238 Mpc, and a standard deviation of 0.102. In addition, the majority of systems have projected separation between 0.12 and 0.35 Mpc with two peaks around 0.21 Mpc, and 0.29 Mpc.

Fig. 1b shows the distribution of the mean harmonic separation with a right-skewed or asymmetric distribution with highest population (73 systems) between 0.1 to 0.2 Mpc and a lowest population (5 systems) with nearly 0.5 Mpc. We also noticed that only 10 systems (3.2%) are compact triplets, with $r_h < 0.04$ Mpc, while the other 305 (96.8%) are wide galaxy triplets ($r_h > 0.04$ Mpc).

Fig. 1c illustrates the distribution of velocity dispersion showing a right-skewed histogram with two peaks with the same number of triplets (28 systems) at the ranges between 30 km s^{-1} to 35 km s^{-1} and 45 km s^{-1} to 50 km s^{-1} , respectively. In addition, most systems fall into velocity dispersion of 20 to 60 km s^{-1} . Only 5 systems have velocity dispersion between 100 and 120 km s^{-1} . There is no occurrence from 105 to 110 km s^{-1} .

Fig. 1d and Fig. 1e represent the distribution of the virial mass and the mass-to-light ratio, respectively. The distribution of virial mass shows a maximum number of

170 systems with virial masses smaller than $10^{12} M_\odot$, and about 75 systems with virial masses between 0.1×10^{13} and $0.2 \times 10^{13} M_\odot$. In contrast, there is no occurrence of systems between 0.8×10^{13} and $1.1 \times 10^{13} M_\odot$, and only 7 systems have virial masses between 1.1×10^{13} to $1.2 \times 10^{13} M_\odot$. This range is wider than that obtained in previous studies (Vavilova et al. 2005).

In order to benchmark our result with previous studies, we compared our computed dynamical parameters with other triplet samples, see Table 3. For comparison we used a list of 176 galaxy triplets from the Local Supercluster (LS) compiled by Vavilova et al. (2005) on the basis of LEDA2003 under the restriction of radial velocity ($v < 3100 \text{ km s}^{-1}$) in the zone $|b| > 10^\circ$, the 156 triplet sample on the basis of LEDA1996 compiled by Makarov & Karachentsev (2000) (MK2000) with a criteria based on the Karachentsev algorithm (Karachentsev 1994), a list of 56 triplets in Tully's catalogue with radial velocity less than 3000 km s^{-1} (Tully 1987), wide triplets compiled by Trofimov & Chernin (1995) with velocity different $< 600 \text{ km s}^{-1}$, SDSS-triplets which composed of 92 triplets with absolute magnitude brighter than $M_r = -20.5$ in the redshift range $0.01 \leq z \leq 0.14$ (Duplancic et al. 2015), K-triplets which composed of 37 compact triplets selected from the original catalogue of Karachentsev et al. (1988) with redshift range $0 \leq z \leq 0.05$ and radial velocity difference $< 500 \text{ km s}^{-1}$ (Duplancic et al. 2015).

From this comparison we found that the median values of our sample are close to those of LS and MK2000 although they are selected under different conditions and criteria. The median of the mass-to-light ratio (M_{vir}/L_r) of our sample is 1.5 times smaller than that of LS and MK2000, and 4-7 times smaller than wide and Tully samples. This is probably due to the small range of apparent magnitude of SIT sample ($11 \leq m_r \leq 15.7$). On the other hand, wide sample shows the largest mean harmonic separation (r_h), and therefore, the largest virial mass (M_{vir}) and mass-to-light ratio (M_{vir}/L). Moreover, the SDSS and the K-triplets have the largest σ , and the smallest r_h because they are identified as compact triplets with small projected separations (r_p). These different ranges are probably due to different selection criteria used to compile these different samples.

Since most of the systems in SIT catalogue are wide (loose), we expect that their properties will match those of loose groups. This expectation has been confirmed after confronting our systems with loose groups in the sample studied by Merchán & Zandivarez (2005).

In addition, we compared the ranges of the dynamical parameters of our triplets sample (σ , M_{vir} , and M_{vir}/L) with more denser groups and clusters, see Table 4. This comparison showed that the ranges of the dynamical parameters increase steeply from low to denser groups and clusters of galaxies. The velocity dispersion starts from 6 km s^{-1} for galaxy triplets up to 2000 km s^{-1} for rich clusters. Whereas, the virial mass increases from $0.01 M_\odot \times 10^{12}$ in case of galaxy triplets up to $3200 M_\odot \times 10^{12}$ for rich clusters. Finally, the mass-to-light ratio shows an ascending manner starting from 0.1 for triplets to reach its maximum at 500 for rich clusters.

Table 1. Ranges of the calculated basic parameters of the member galaxies in the studied sample of triplets

Parameters (members)	Units	Range	
		Min.	Max.
Radial velocity (v)	$km\ s^{-1}$	1819.7	24010.3
Projected separation (r_p)	Mpc	0.009	0.847
Absolute magnitude in r-band (M_r)	–	-22.8	-14.5
Luminosity (L_r)	L_\odot	4.7×10^7	9.7×10^{10}

Table 2. Statistical parameters calculated for the 315 triplet systems selected from the SIT catalogue. STD refers to the standard deviation

Parameters (systems)	Units	Range		Statistical Parameters		
		Min.	Max.	Median	Mean	STD
Velocity dispersion (σ)	$km\ s^{-1}$	6.2	123.6	43.8	45.4	21.9
Mean harmonic separation (r_h)	Mpc	0.017	0.508	0.17	0.19	0.10
Virial Mass (M_{vir})	M_\odot	10.0×10^9	1.2×10^{13}	1.5×10^{12}	1.5×10^{12}	1.8×10^{12}
Mass-to-Light ratio (M_{vir}/L_r)	–	0.1	308	41.4	41.4	50.6

Table 3. Comparison between the median values of the dynamical parameters (σ , r_h , M_{vir} , M_{vir}/L_r) of our sample and other triplet samples. NTS refers to the Number of Triplet Systems

Sample	NTS	σ ($km\ s^{-1}$)	r_h (kpc)	M_{vir} ($M_\odot \times 10^{12}$)	(M_{vir}/L_r) (M_\odot/L_\odot)	References
SIT	315	44	166	1.50	23	This work
LS	176	30	160	0.36	35	Vavilova et al. (2005)
MK2000	156	33	178	0.52	35	Makarov & Karachentsev (2000)
Tully	56	56	269	2.63	111	Tully (1987)
Wide	37	66	396	4.47	173	Trofimov & Chernin (1995)
SDSS	92	119	67	1.00	–	Duplancic et al. (2015)
K-triplets	37	114	54	1.00	–	Duplancic et al. (2015)

3.2 Satellite-to-central galaxy parameters ratios

In Fig. 2, we illustrate the ratio of both absolute magnitude (M_r), panel a, and luminosity (L_r), panel b, in the r-band for the primary galaxy (G1), the brightest in the system, and the two satellite galaxies G2 and G3. It is notable that the absolute magnitude ratio of G2/G1 (solid line) has a mean value of 1/1.06, while that for G3/G1 (dashed line) is 1/1.12. Similarly, the luminosity of G2/G1 (solid line) has a mean value of 1/3.45 and that of G3/G1 (dashed line) is 1/7.7. Thus, both the absolute magnitude and the luminosity ratio of G3/G1 are much smaller than those of G2/G1. This indicates that isolated triplets usually show a hierarchical structure, and it is less probably to find a triplet system with two similar absolute magnitude and luminosity for its members. We conclude that in triplets the central (primary) galaxy is always brighter and more luminous than the two satellite galaxies. These results are in line with Argudo-Fernández et al. (2015) findings in which the typical satellite-to-primary mass ratio is 1/100. They also found that the central galaxy is the most massive galaxy of the three members in the triplet system. The statistical parameters of the absolute magnitude and luminosity ratios are summarised in Table 5.

3.3 Correlations of the mean separation between triplet members (\bar{r}_p) with the systems dynamical parameters (σ , M_{vir} , M_{vir}/L_r)

Correlation coefficients quantify the correlation between two or more random variables measured for a system of galaxies. In this study, we examined the correlation between the dynamical parameters (σ , M_{vir} , M_{vir}/L_r) and the mean values of the projected separations, r_p , (see Figs. 3, 4, and 5) by estimating their correlation coefficients.

Fig. 3 demonstrate the relationship between the velocity dispersion (σ) and \bar{r}_p . It is clear that there is no correlation between σ and \bar{r}_p ($f_{r_p\sigma} = -0.03$). We also found that the compact systems, in this catalogue, are distributed at lower \bar{r}_p indicating that \bar{r}_p decreases directly with r_h . In addition, the majority of these systems are concentrated at lower σ , smaller than $60\ km\ s^{-1}$.

The correlation of M_{vir} with \bar{r}_p , in Fig. 4, shows a random distribution with a weak correlation coefficient ($f_{r_p M_{vir}} = 0.37$). Compact systems tend to be concentrated in a small range of M_{vir} ($0.004 \leq M_{vir} (\times 10^{13} M_\odot) \leq 0.11$) and show a nearly linear relation with \bar{r}_p .

Fig. 5 illustrates the marginal correlation between \bar{r}_p and M_{vir}/L_r with $f_{r_p M_{vir}/L_r} = 0.06$. It is hard to identify a specific relation from this random distribution. However, we

Table 4. Comparison between the ranges of the dynamical parameters (σ , M_{vir} , M_{vir}/L_r) of galaxy triplets in our study and more denser groups and clusters of galaxies. NG is the number of galaxies in a given system, group, or cluster.

Sample	NG	size Mpc	σ ($km\ s^{-1}$)	M_{vir} ($M_{\odot} \times 10^{12}$)	(M_{vir}/L_r) (M_{\odot}/L_{\odot})	References
SIT	3	1	6-124	0.01-10	0.1-308	This work
groups	< 50	2	150-500	20-32	300-400	Carroll & Ostlie (2006); Bohringer (2007)
clusters	50-1000	6-8	800-2000	1000-3200	>500	Carroll & Ostlie (2006); Bohringer (2007)

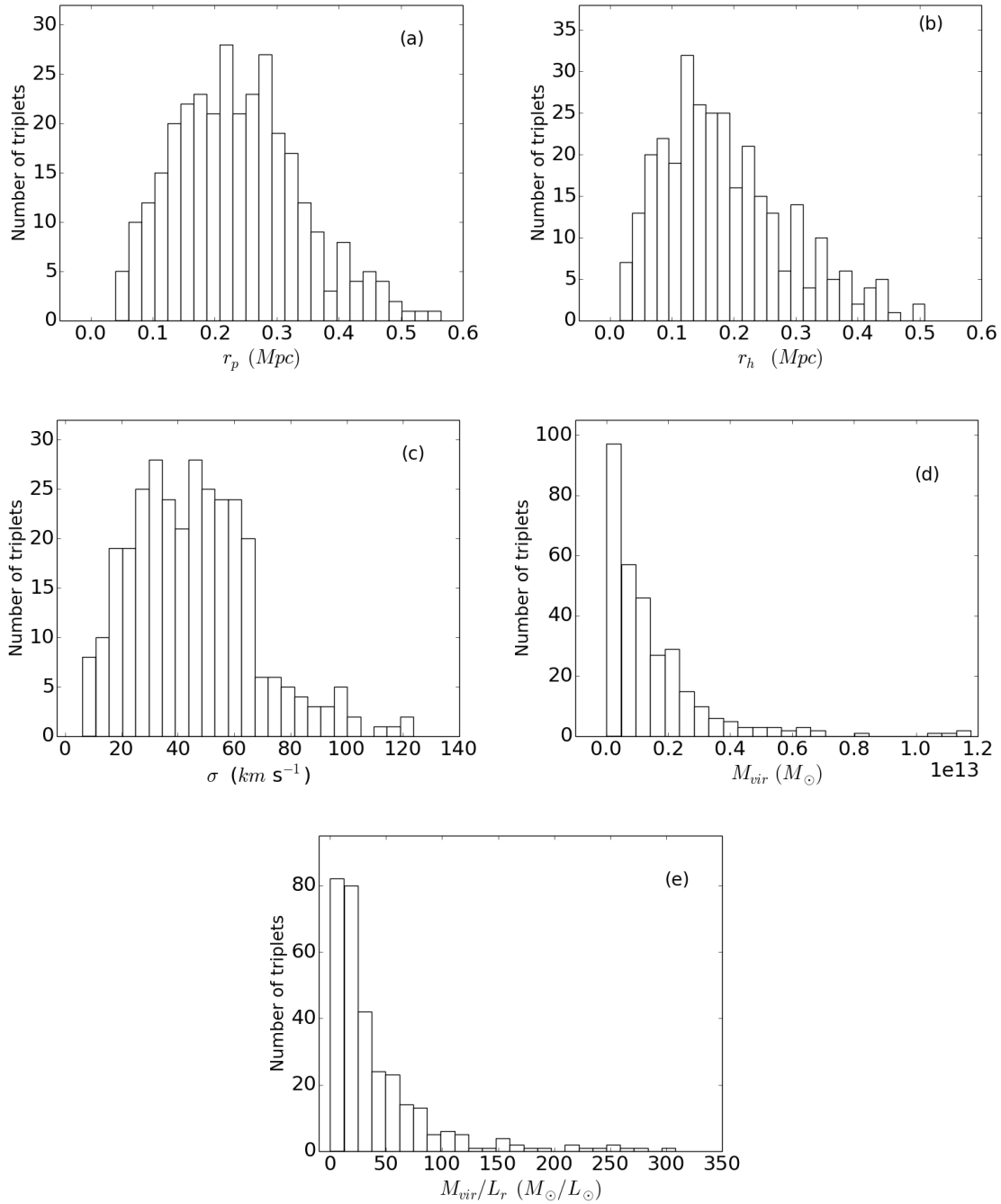
**Figure 1.** Histograms represent the distribution of the computed parameters for triplet systems and their members. (a) the projected separation (r_p), (b) the mean harmonic separation (r_h), (c) the velocity dispersion (σ), (d) the virial mass (M_{vir}), and (e) the mass-to-light ratio (M_{vir}/L_r)

Table 5. Statistical values for the ratios of absolute magnitude (M_r) and luminosity (L_r) in the r-band of the satellite galaxies (G2 and G3) to those of the primary galaxy (G1). STD refers to the standard deviation.

Parameters	Range		Statistical Values		
	Min.	Max.	Median	Mean	STD
M_{rG2}/M_{rG1}	0.76	1.00	0.94	0.94	0.04
M_{rG3}/M_{rG1}	0.67	0.98	0.89	0.89	0.05
L_{rG2}/L_{rG1}	0.01	1.03	0.37	0.29	0.25
L_{rG3}/L_{rG1}	0.001	0.71	0.16	0.13	0.12

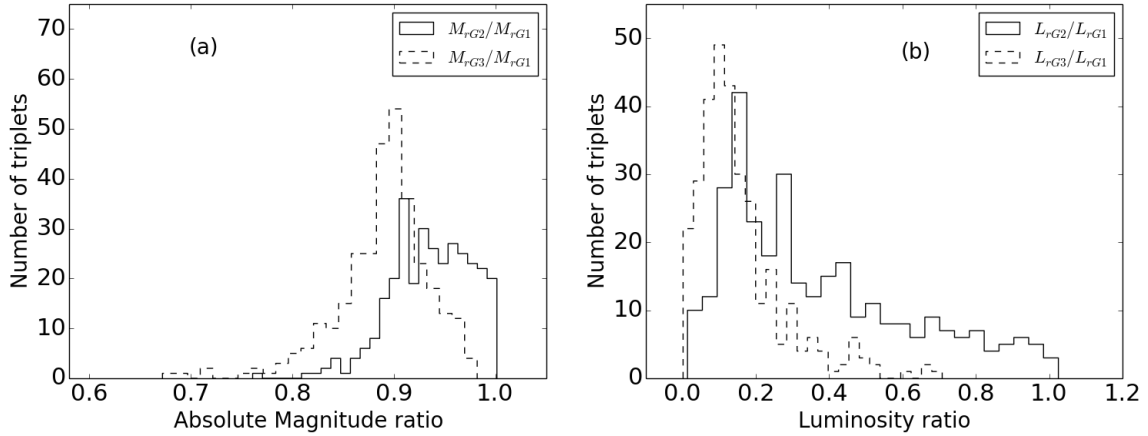


Figure 2. The ratio between the absolute magnitude (M_r), panel a, and the luminosity (L_r), panel b, between the galaxies G2 and G1 (solid lines) and G3 and G1 (dashed lines) for the studied SIT sample.

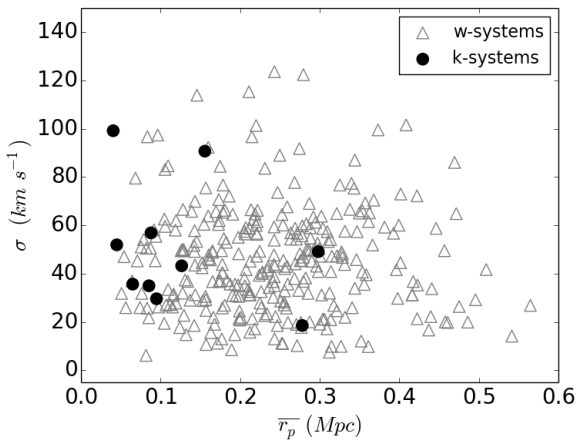


Figure 3. Correlation between the velocity dispersion (σ) and the mean projected separation (\bar{r}_p) for the 315 triplet systems of SIT catalogue. Circles represent the ten compact systems (k-systems), while triangles represent the wide systems (w-systems) of this sample, as shown in the legend.

found that compact systems (solid circles) are concentrated at lower M_{vir}/L_r ($0.84 \leq M_{vir}/L_r \leq 90.03$) compared to wide systems (open triangles).

The weak correlations obtained indicate that triplets in this catalogue follow the characteristics and properties of

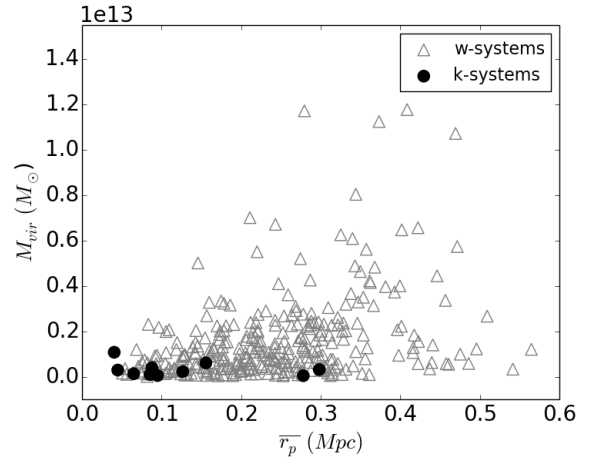


Figure 4. Correlation of virial mass (M_{vir}) with mean projected separation (\bar{r}_p) for the 315 triplet systems of SIT. Symbols are the same as in Fig. 3a.

Tully (Tully 1987) and Wide triplets (Trofimov & Chernin 1995) confirming that these systems are far from the state of virial equilibrium since they have the largest mean harmonic separations and mass-to-light ratios that is in-line with Vavilova et al. (2005). Hence, we may conclude that merging is hard to take place between members of such wide triplet systems.

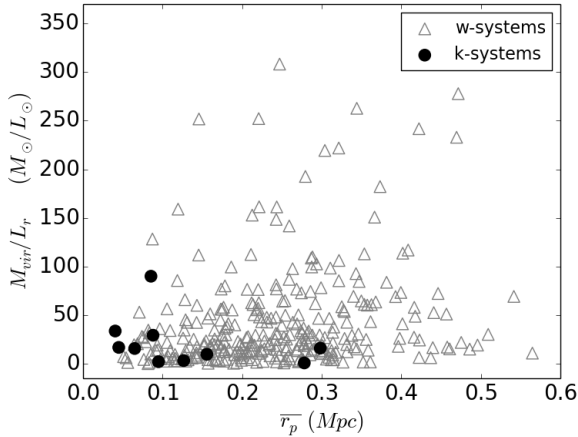


Figure 5. Correlation of mass-to-light ratio (M_{vir}/L_r) with mean projected (\bar{r}_p) separation for the wide (w, triangles) and the compact (k, circles) systems in our sample.

In addition, we found that compact systems have nearly constant M_{vir} along the variation of \bar{r}_p and are characterised by small values of M_{vir} and M_{vir}/L_r . They are always fall at the small range ($0.04 \leq \bar{r}_p \leq 0.3$). This defines the small halo where members of compact systems are embedded.

3.4 Correlations between triplets dynamical parameters and the Large-Scale Structure (LSS)

Argudo-Fernández et al. (2015) specified in their final primary isolated galaxy triplets sample to have radial velocity differences range $-500 \leq \Delta v \leq 500 \text{ km s}^{-1}$ (and within 1 Mpc). They have also characterised the Large-Scale Structure (LSS) around each primary galaxy (G1) to be $d_{NN} \leq 5$ Mpc, where d_{NN} denotes the distance to the first nearest neighbour from G1 and is specified to be from 1 to 5 Mpc in their criteria. They, also, defined the average density along line of sight through the LSS as the projected number density parameter ($\eta_{k,LSS}$) and the tidal strength generated by the galaxies in the LSS (Q_{LSS}). These parameters are quantified to investigate the effect of the LSS environment on the properties of triplet galaxies. Hence, it is important to explore the correlation between d_{NN} (in Mpc), $\eta_{k,LSS}$ and Q_{LSS} and the triplets' dynamical parameters (σ , r_h , M_{vir} , and M_{vir}/L_r); see Figures 6, 7 and 8. In addition, the relation between the tidal strength (Qt), defined as the total gravitational interaction strength produced by the neighbour galaxies (G2 and G3) on the central galaxy (G1), and the triplets dynamical parameters has been investigated (Fig. 9).

The correlation between the distance from G1 to the first nearest neighbour of the LSS (d_{NN}) in Mpc and the velocity dispersion (σ), the mean harmonic separation (r_h), the virial mass (M_{vir}), and the mass-to-light ratio (M_{vir}/L_r) of the 313 triplet systems (after excluding the two systems (SIT 99 and SIT 168) mentioned before in Sec. 2.2) is illustrated in Fig. 6. It is clear that there is no correlation between d_{NN} and the dynamical parameters of the studied sample, where the correlation coefficients were found to be

0.018, -0.06, -0.075, and -0.0013, respectively. Interestingly, we found that most of compact systems (8 from 10) are located at lower σ ($18.5 \leq \sigma \leq 56.9$) and are all concentrated toward smaller M_{vir} , and M_{vir}/L_r . M_{vir} of compact systems have nearly the same value representing an almost linear distribution with the LSS parameters. They are always occupied the d_{NN} range $1.1 \leq d_{NN} \leq 2.4$ indicating that the probability of an isolated triplet system to have neighbours increases in compact systems. This means that wide triplets seems to be more isolated than compact triplets.

Similarly, Figs. 7, and 8, show a poor correlation between Q_{LSS} and $\eta_{k,LSS}$ with σ , r_h , M_{vir} , and M_{vir}/L_r where we obtained correlation coefficients with Q_{LSS} of 0.055, 0.089, 0.094, and 0.049, respectively, and 0.036, 0.058, 0.076, and 0.015, respectively with $\eta_{k,LSS}$. Compact systems are always fall in the range $-6 \leq Q_{LSS} \leq -3$, and $-1.7 \leq \eta_{k,LSS} \leq -0.5$, and follow the same dynamical characteristics as mentioned in their correlation with d_{NN} .

Generally, triplet systems are more popular at lower values of M_{vir} and M_{vir}/L_r with all LSS parameters d_{NN} , $\eta_{k,LSS}$, and Q_{LSS} .

In Fig. 9, Qt does not show any relation neither with σ ($f_{Qt\sigma} = 0.074$), M_{vir} ($f_{QtM_{vir}} = -0.234$), nor with M_{vir}/L_r ($f_{QtM_{vir}/L_r} = -0.0247$). We observed that the scattering is more pronounced at lower Qt (≤ -2) and compact systems are concentrated at higher Qt (> 0) except one system at $Qt = -2$. This means that tidal strength in compact systems is larger than that in wide systems; i.e. compact systems are more bounded than wide systems. On the other hand, a fair negative correlation between Qt and r_h is found with $f_{QLSSr_h} = -0.614$ and can be expressed by the following equation

$$r_h = -0.057(\pm 0.004) \times Qt + 0.088. \quad (11)$$

Discussions of Figs. 6 and 8 indicate that all galaxy triplets in the studied catalogue are perfectly isolated, and hence has no relation with the LSS. On the other hand, Qt shows a relation with only r_h (see Fig. 9) which means that as the gravitational radius between the members of a triplet system increases, the tidal strength between the triplet galaxies decreases, and vice-versa. Thus suggesting that the dynamical evolution in isolated triplets is mainly due to the galaxies within the same halo and it does not depend on the location of the system in the LSS. This result is supported by the findings of Argudo-Fernández et al. (2015) in which they found that isolated triplets have a common origin in their formation and evolution and most of them belong to the outer parts of filaments, walls, and clusters, and they are not located in voids.

4 CONCLUSIONS

We carried out a statistical study on 315 triplet systems chosen from the recently published catalogue of isolated galaxy triplets ‘‘SDSS-based catalogue of Isolated Triplets’’ (SIT), (Argudo-Fernández et al. 2015). For these systems and their members, we computed the physical (radial velocities (v), angular separations (θ), projected separations (r_p), luminosity (L_r), and absolute magnitudes (M_r)) as well as the

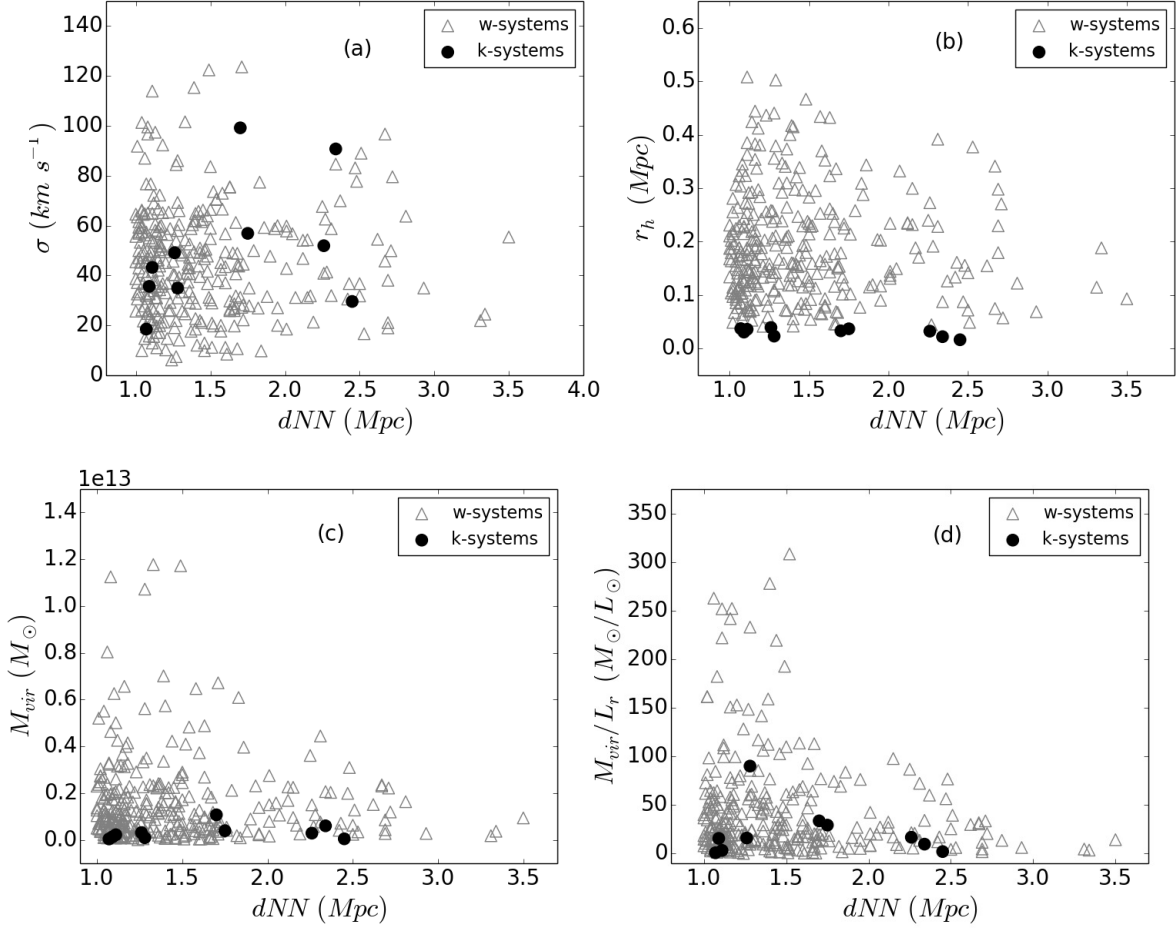


Figure 6. Distance from the brightest galaxy to the first neighbour (d_{NN}) plotted versus (a) velocity dispersion (σ), (b) mean harmonic separation (r_h), (c) virial mass (M_{vir}), and (d) mass-to-light ratio (M_{vir}/L_r) for the 313 galaxy triplet systems. Wide and compact systems are categorised as shown in the legend.

dynamical (velocity dispersion (σ), the mean harmonic separation (r_h), virial masses (M_{vir}/M_\odot), and mass-to-light ratios (M_{vir}/L_r)) parameters. We then distinguished between wide and compact triplet systems by estimating their mean harmonic separation (r_h). In addition, we investigated the correlation between the estimated parameters and the triplets parameters given in the published catalogue. From the results of this study we may summaries our main conclusions as follows:

1. It is difficult to predict merging between members of triplet systems, in this study, as a step through their evolution.
2. The selected catalogue includes only 3.2% compact systems and the rest are wide which might be the main reason that we found larger median values of physical and dynamical parameters than other previous studies.
3. Denser groups (> 3 members) and clusters possess higher values of dynamical parameters.
4. SIT systems are more bounded (high tidal strength) at lower values of gravitational radii (r_h).
5. Compact systems in SIT catalogue record the smallest mean values of dynamical parameters, comparing to K-

triplet sample. This may imply that SIT compact systems are special and further investigation of such systems in other catalogues is required for future work.

6. SIT systems are perfectly isolated from their surrounding. This indicates that their dynamical evolution is independent of their location in the Universe, but depends on the evolution of the systems' own members. Therefore, we may confirm that isolated triplets have a common origin in their formation and evolution and most of them belong to the outer parts of filaments, walls, and clusters, and they are not located in voids similar to the findings by [Argudo-Fernández et al. \(2015\)](#).

7. Parameters of primary (G1) and satellite galaxies (G2 and G3) show that G1 is always brighter and more luminous than G2 and G3. This confirms the hierarchical structure of isolated triplets ([Hernández-Toledo et al. 2011](#); [Argudo-Fernández et al. 2015](#); [Duplancic et al. 2015](#)).

The most important thesis beyond this work is to highlight the importance of statistical studies of galaxy triplets as a first essential step toward understanding the formation and evolution of groups and large scale structures. More analysis of these poorly populated systems such as decompo-

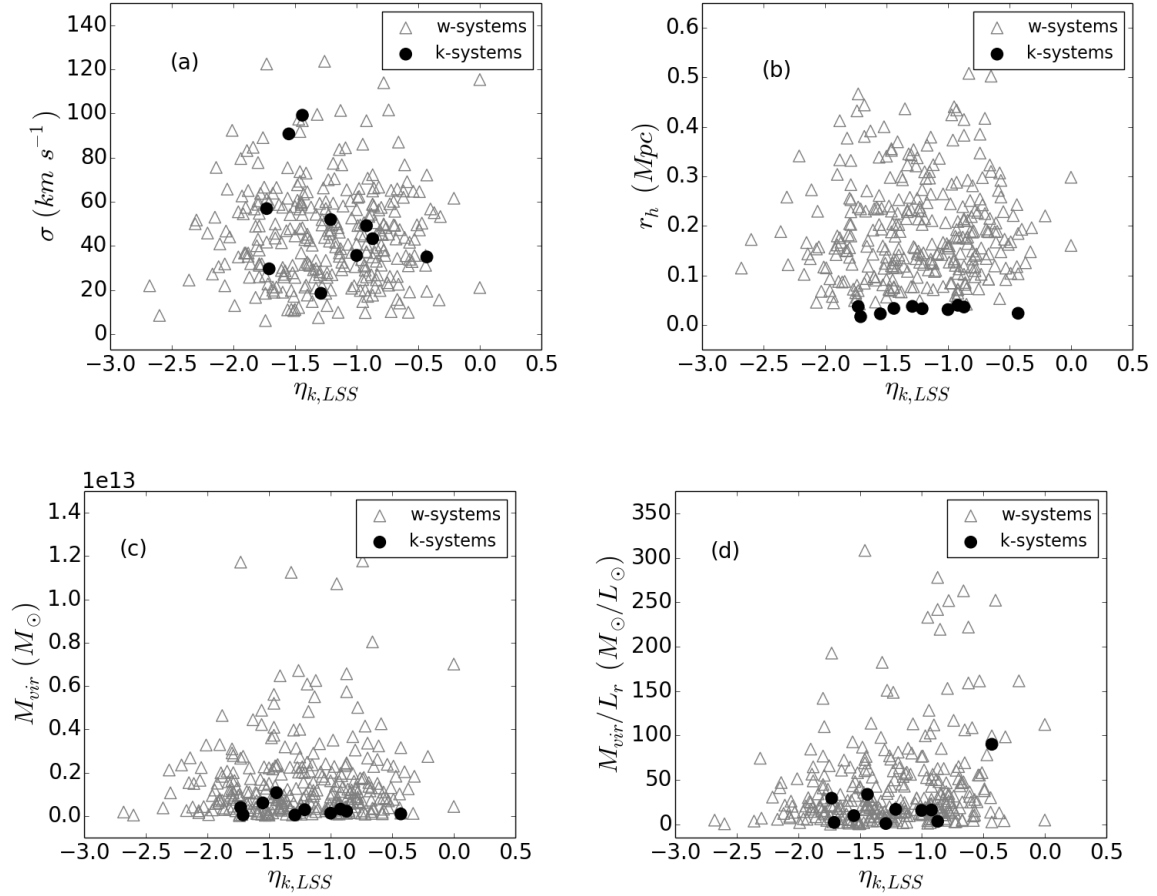


Figure 7. Scatter plots between projected density of the LSS ($\eta_{k,LSS}$) and (a) velocity dispersion (σ), (b) mean harmonic separation (r_h), (c) virial mass (M_{vir}), and (d) mass-to-light ratio (M_{vir}/L_r) for the 313 galaxy triplet systems. Circles represent the ten compact systems (k-systems), while triangles represent the wide systems (w-systems) of this sample.

sition and photometric studies are requested for better understanding of their properties. These further analyses are kept for our future work.

ACKNOWLEDGEMENTS

This work was impossible to present without the effort made by our colleague Gamal Bakr Ali who passed away just before submitting this work. We dedicate this work for his soul.

Amira A. Tawfeek thanks Samuel Boissier³ and Henri Plana⁴, for their helpful comments and suggestions, during a scientific visit to the Laboratoire d’Astrophysique de Marseille (LAM) that improved this work. Amira A. Tawfeek also thanks Sonali Sachdeva⁵ for her great effort in im-

proving the abstract in our manuscript, during her scientific visit to the Inter-University Centre for Astronomy and Astrophysics.

Funding for SDSS-III has been provided by the Alfred P. Sloan Foundation, the Participating Institutions, the National Science Foundation, and the U.S. Department of Energy Office of Science. The SDSS-III web site is <http://www.sdss3.org/>.

SDSS-III is managed by the Astrophysical Research Consortium for the Participating Institutions of the SDSS-III Collaboration including the University of Arizona, the Brazilian Participation Group, Brookhaven National Laboratory, Carnegie Mellon University, University of Florida, the French Participation Group, the German Participation Group, Harvard University, the Instituto de Astrofísica de Canarias, the Michigan State/Notre Dame/JINA Participation Group, Johns Hopkins University, Lawrence Berkeley National Laboratory, Max Planck Institute for Astrophysics, Max Planck Institute for Extraterrestrial Physics, New Mexico State University, New York University, Ohio State University, Pennsylvania State University, University of Portsmouth, Princeton University, the Spanish Partic-

³ (samuel.boissier@lam.fr) [Laboratoire d’Astrophysique de Marseille, France]

⁴ (plana@uesc.br) [Laboratorio de Astrofísica Teórica e Observacional, Universidade Estadual de Santa Cruz - 45650-000, Ilheus-BA, Brazil]

⁵ (sonali@iucaa.in) [Inter-University Centre for Astronomy and Astrophysics (IUCAA), Pune, India]

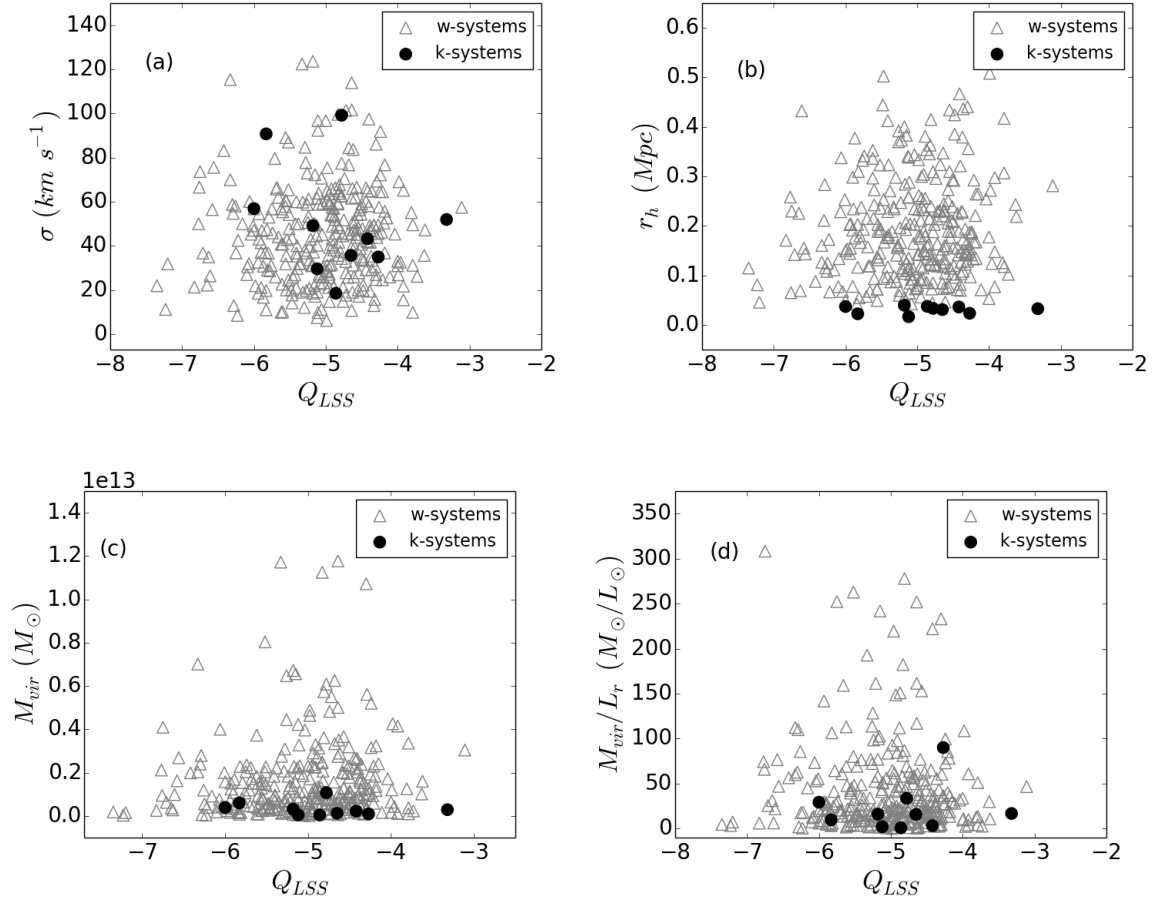


Figure 8. Scatter plots between tidal strength estimation of the LSS (Q_{LSS}) and (a) velocity dispersion (σ), (b) mean harmonic separation (r_h), (c) virial mass (M_{vir}), and (d) mass-to-light ratio (M_{vir}/L_r) for the 313 galaxy triplets systems. Symbols are the same like in Fig. 7.

ipation Group, University of Tokyo, University of Utah, Vanderbilt University, University of Virginia, University of Washington, and Yale University.

REFERENCES

- Ahn C. P., et al., 2014, *ApJS*, **211**, 17
 Alam S., et al., 2015a, *ApJS*, **219**, 12
 Alam S., et al., 2015b, *ApJS*, **219**, 12
 Ali G., 2001, in *On the Physical and Geometrical Properties of Paired and Interacting Galaxies*, PhD thesis, Cairo University, Faculty of Science.
 Argudo-Fernández M., et al., 2015, *A&A*, **578**, A110
 Bahcall N. A., 1996, ArXiv astro-ph/9611148,
 Bilir S., Karaali S., Tunçel S., 2005, *Astronomische Nachrichten*, **326**, 321
 Binney J., Tremaine S., 1987, *Nature*, **326**, 219
 Blanton M. R., et al., 2003, *ApJ*, **592**, 819
 Bohringer H., 2007, *The Universe in X-Rays*. Vol. 23
 Carroll B. W., Ostlie D. A., 2006, *An introduction to modern astrophysics and cosmology*
 Chernin A. D., Ivanov A. V., Trofimov A. V., Mikkola S., 1994, *A&A*, **281**, 685
 Chernin A. D., Dolgachev V. P., Domozhilova L. M., 2000, *MNRAS*, **319**, 851
 Dekel A., Ostriker J. P., 1999, in *Cambridge University Press ed., Formation of Structure in the Universe*. p. 164
 Duplancic F., O’Mill A. L., Lambas D. G., Sodr  L., Alonso S., 2013, *MNRAS*, **433**, 3547
 Duplancic F., Alonso S., Lambas D. G., O’Mill A. L., 2015, *MNRAS*, **447**, 1399
 Feng S., Shao Z.-Y., Shen S.-Y., Argudo-Fern ndez M., Wu H., Lam M.-I., Yang M., Yuan F.-T., 2016, *Research in Astronomy and Astrophysics*, **16**, 72
 Hern ndez-Toledo H. M., M ndez-Hern ndez H., Aceves H., Olgu n L., 2011, *AJ*, **141**, 74
 Hickson P., 1977a, *ApJ*, **217**, 16
 Hickson P., 1977b, *ApJ*, **217**, 964
 Karachentsev I., 1994, *Astronomical and Astrophysical Transactions*, **6**, 1
 Karachentsev I. D., Karachentseva V. E., 1981, *Astrofizika*, **17**, 5
 Karachentsev V. E., Karachentsev I. D., Lebedev V. S., 1988, *Astrofizicheskie Issledovaniia Izvestiya Spetsial’noj Astrofizicheskoy Observatorii*, **26**, 37
 Karachentseva V. E., Karachentsev I. D., Shcherbanovskiy A. L., 1979, *Astrofizicheskie Issledovaniia Izvestiya Spetsial’noj Astrofizicheskoy Observatorii*, **11**, 3

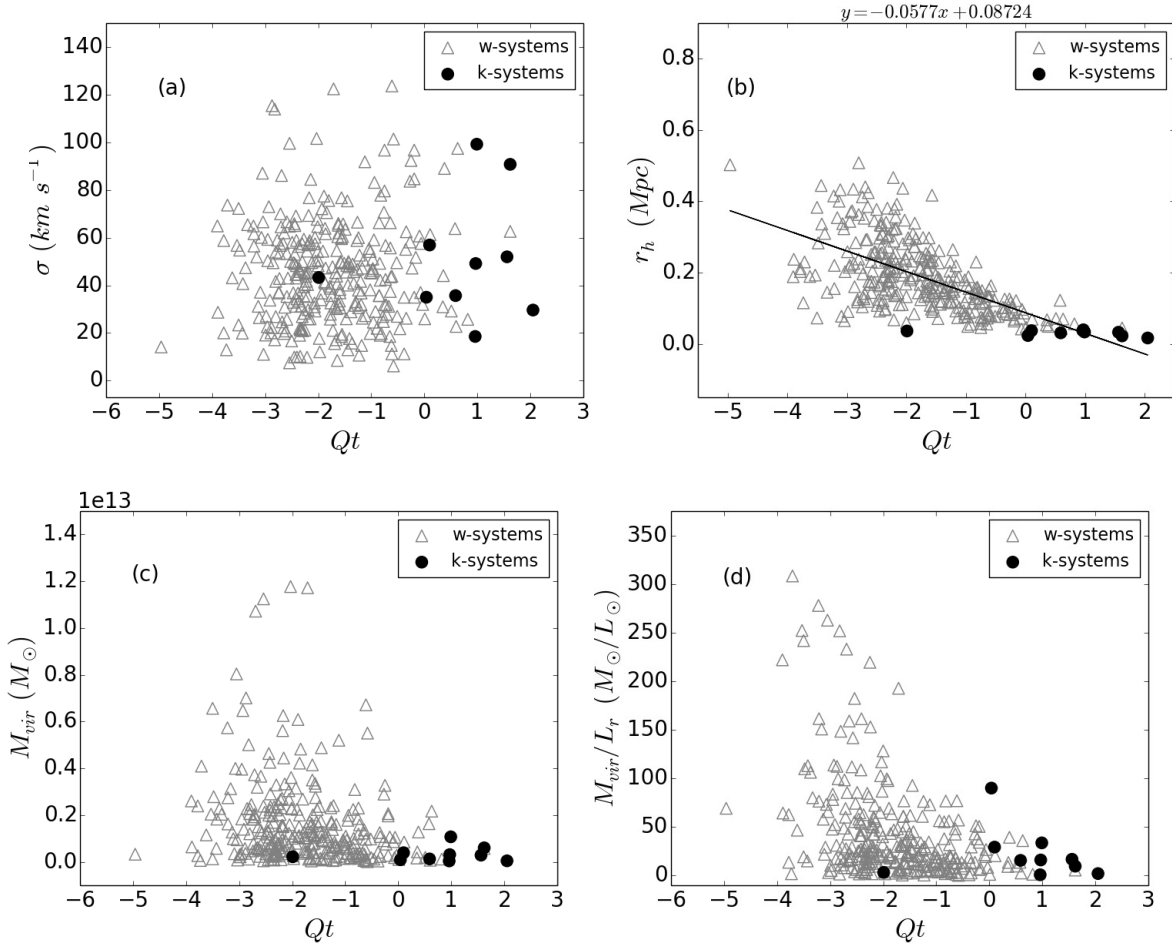


Figure 9. Correlation between tidal strength estimated on the galaxy (G1) exerted by the G2 and G3 galaxies (Qt) and (a) velocity dispersion (σ), (b) mean harmonic separation (r_h), (c) virial mass (M_{vir}), and (d) mass-to-light ratio (M_{vir}/L_r) for the galaxy triplet systems. Circles represent the ten compact systems (k-systems), while triangles represent the wide systems (w-systems) of this sample.

Kiseleva L., 2000, in Valtonen M. J., Flynn C., eds, *Astronomical Society of the Pacific Conference Series Vol. 209, IAU Colloq. 174: Small Galaxy Groups*. p. 388

Liljeblad E., 2012, in E.Liljeblad ed., *Estimating masses of galaxy clusters*. pp 3–5

Makarov D. I., Karachentsev I. D., 2000, in Valtonen M. J., Flynn C., eds, *Astronomical Society of the Pacific Conference Series Vol. 209, IAU Colloq. 174: Small Galaxy Groups*. p. 40 ([arXiv:astro-ph/9909343](https://arxiv.org/abs/astro-ph/9909343))

Merchán M. E., Zandivarez A., 2005, *ApJ*, **630**, 759

O’Mill A. L., Duplancic F., García Lambas D., Valotto C., Sodrè L., 2012, *MNRAS*, **421**, 1897

Patton D. R., Ellison S. L., Simard L., McConnachie A. W., Mendel J. T., 2011, *MNRAS*, **412**, 591

Rodgers C. T., Cantnera R., Smith J. A., Pierce M. J., Tucker D. L., 2006, *AJ*, **132**, 989

Schneider P., 2006, in *Extragalactic Astronomy and Cosmology*.

Shen S.-Y., et al., 2016, *Research in Astronomy and Astrophysics*, **16**, 43

Smart W. M., 1965, *Text-book on spherical astronomy*

Trofimov A. V., Chernin A. D., 1995, *Azh*, **72**, 308

Tully R. B., 1987, *ApJ*, **321**, 280

Valtonen M. J., Mikkola S., 1991, in *Bulletin of the American Astronomical Society*. p. 1393

Vavilova I. B., Karachentseva V. E., Makarov D. I., Melnyk O. V., 2005, *Kinematika i Fizika Nebesnykh Tel*, **21**, 3

APPENDIX A:

In the following, we show three images of compact triplet systems, in Fig. A1, and three images of wide triplet systems (Fig. A2) from the selected catalogue. In addition, Table A1 lists the main computed parameters for the 315 studied galaxy triplet systems⁶. The columns of the Table are: Index for the systems, position (RA, DEC) of the brightest galaxy in the system, redshift (z), velocity dispersion (σ), virial mass (M_{vir}), mass-to-light ratio (M_{vir}/L_r), mean projected separation (r_p), mean harmonic separation (r_h), and finally a flag indicating the status of compact system (k) and wide (w) triplet.

This paper has been typeset from a $\text{\TeX}/\text{\LaTeX}$ file prepared by the author.

⁶ k represents compact systems and w represents wide systems

Table A1. Computed basic parameters of the 315 studied triplet systems in the SIT catalogue . The flag in the last column is (k) for compact galaxy triplets and (w) for wide systems

Index	RA	DEC	z	σ $km\ s^{-1}$	M_{vir} $10^{12}M_{\odot}$	M_{vir}/L_r M_{\odot}/L_{\odot}	\bar{r}_p Mpc	r_h Mpc	flag
1	171.315	-2.076	0.063	16.66	0.03	6.19	0.44	0.38	w
2	208.677	65.244	0.036	63.5	0.24	61.87	0.29	0.18	w
3	211.203	4.981	0.046	66.47	0.17	60.9	0.21	0.12	w
4	251.468	44.437	0.07	45.82	0.24	30.57	0.35	0.34	w
5	133.535	0.499	0.028	20.04	0.03	13.65	0.29	0.2	w
6	207.824	0.385	0.03	29.0	0.02	5.86	0.14	0.05	w
7	218.956	62.421	0.048	61.6	0.42	43.3	0.36	0.34	w
8	197.686	0.032	0.041	33.77	0.14	52.57	0.44	0.37	w
9	320.876	-7.746	0.028	49.5	0.09	26.36	0.13	0.11	w
10	22.224	14.721	0.037	83.66	0.29	42.87	0.23	0.13	w
11	127.46	48.781	0.024	14.75	0.01	4.04	0.13	0.12	w
12	200.92	1.362	0.057	49.22	0.1	11.19	0.14	0.13	w
13	232.209	0.777	0.04	9.89	0.01	1.68	0.33	0.3	w
14	225.273	0.53	0.036	59.98	0.14	76.37	0.22	0.12	w
15	259.779	65.732	0.036	25.94	0.04	29.49	0.23	0.2	w
16	192.983	-2.078	0.023	18.53	0.02	8.58	0.25	0.14	w
17	155.232	1.236	0.071	97.43	0.22	36.0	0.1	0.07	w
18	190.146	2.468	0.046	47.74	0.09	16.36	0.16	0.12	w
19	211.262	-0.251	0.033	56.9	0.04	29.31	0.09	0.04	k
20	189.952	-2.796	0.048	31.19	0.1	17.13	0.3	0.3	w
21	231.978	54.27	0.04	19.79	0.02	4.67	0.26	0.16	w
22	134.774	53.772	0.008	22.61	0.04	47.78	0.23	0.22	w
23	145.6	63.165	0.031	50.01	0.21	74.37	0.29	0.26	w
24	119.168	44.87	0.05	55.08	0.13	12.81	0.2	0.13	w
25	134.242	52.066	0.013	56.46	0.16	76.55	0.21	0.16	w
26	136.146	52.12	0.066	76.72	0.63	58.63	0.33	0.32	w
27	143.99	54.993	0.059	86.07	1.07	233.0	0.47	0.44	w
28	122.384	39.888	0.064	57.56	0.32	42.68	0.33	0.29	w
29	162.281	4.941	0.055	77.77	0.31	76.78	0.27	0.16	w
30	348.122	13.942	0.034	31.82	0.02	4.39	0.08	0.07	w
31	143.019	51.551	0.034	36.74	0.18	48.82	0.42	0.41	w
32	138.259	49.639	0.013	20.82	0.02	16.4	0.2	0.17	w
33	148.124	2.154	0.017	26.96	0.02	7.43	0.11	0.08	w
34	310.094	-6.359	0.036	29.78	0.09	26.14	0.4	0.32	w
35	188.066	3.0	0.044	57.53	0.11	26.86	0.21	0.1	w
36	25.882	13.514	0.054	48.89	0.12	19.69	0.17	0.15	w
37	136.811	2.443	0.051	61.26	0.09	20.41	0.29	0.07	w
38	206.814	62.47	0.044	27.26	0.02	5.67	0.11	0.1	w
39	323.223	-7.197	0.061	101.35	0.55	57.14	0.22	0.16	w
40	186.865	3.302	0.049	24.52	0.04	3.61	0.2	0.19	w
41	176.138	61.534	0.048	92.34	0.33	51.3	0.16	0.12	w
42	174.362	1.535	0.046	54.53	0.15	29.93	0.18	0.15	w
43	157.973	62.401	0.052	63.89	0.11	18.02	0.16	0.08	w
44	126.862	41.495	0.036	12.95	0.01	2.65	0.18	0.15	w
45	351.251	-0.002	0.034	51.94	0.03	16.8	0.04	0.03	k
46	208.032	5.432	0.079	26.85	0.12	10.93	0.56	0.51	w
47	233.29	-1.866	0.028	54.75	0.28	109.9	0.29	0.28	w
48	229.519	3.49	0.068	115.36	0.7	112.37	0.21	0.16	w
49	202.904	61.628	0.044	31.19	0.11	27.28	0.42	0.33	w
50	215.19	58.699	0.046	28.86	0.04	11.47	0.15	0.14	w
51	132.899	47.558	0.029	49.46	0.1	13.5	0.13	0.12	w
52	4.924	0.376	0.041	29.2	0.02	9.82	0.16	0.07	w
53	210.055	3.424	0.035	60.67	0.09	21.56	0.28	0.07	w
54	183.633	4.435	0.077	32.6	0.04	2.41	0.23	0.12	w
55	120.005	28.742	0.041	65.42	0.2	80.12	0.18	0.14	w
56	168.342	61.447	0.068	54.13	0.23	32.38	0.31	0.24	w
57	172.764	62.305	0.033	45.33	0.06	19.2	0.09	0.08	w
58	184.541	62.802	0.05	58.97	0.25	29.48	0.29	0.21	w
59	181.213	63.132	0.04	76.72	0.32	36.44	0.18	0.17	w
60	123.241	36.255	0.008	11.22	0.0	3.36	0.17	0.08	w
61	123.449	37.05	0.031	38.24	0.11	31.84	0.28	0.23	w
62	171.927	55.921	0.019	25.94	0.02	28.11	0.07	0.07	w
63	249.554	40.173	0.037	49.04	0.2	55.19	0.33	0.25	w
64	180.241	59.385	0.033	113.93	0.5	251.83	0.15	0.12	w
65	181.569	61.154	0.052	9.79	0.01	1.82	0.36	0.29	w
66	166.865	53.988	0.06	34.99	0.03	6.26	0.21	0.07	w
67	208.745	46.945	0.028	36.74	0.06	25.53	0.17	0.14	w
68	354.18	13.674	0.062	49.95	0.22	33.63	0.28	0.27	w
69	231.268	4.83	0.022	50.01	0.09	45.21	0.13	0.11	w
70	347.753	13.632	0.023	42.47	0.04	18.22	0.15	0.07	w
71	139.105	42.992	0.009	34.99	0.01	90.03	0.09	0.02	k
72	162.697	6.099	0.042	35.3	0.16	24.4	0.42	0.38	w
73	165.592	6.077	0.022	53.87	0.23	148.5	0.24	0.24	w
74	167.143	8.737	0.072	66.24	0.22	37.93	0.18	0.16	w
75	156.429	45.348	0.044	29.61	0.0	2.09	0.09	0.02	k
76	166.154	6.395	0.032	21.34	0.03	19.05	0.22	0.2	w
77	170.689	7.52	0.042	49.46	0.13	34.62	0.17	0.16	w

Table A1. - continued

Index	RA	DEC	z	σ $km\ s^{-1}$	M_{vir} $10^{12}M_{\odot}$	M_{vir}/L_r M_{\odot}/L_{\odot}	\bar{r}_p Mpc	r_h Mpc	flag
78	168.526	55.711	0.028	36.74	0.08	24.75	0.24	0.18	w
79	199.903	-2.912	0.023	49.46	0.23	99.59	0.29	0.28	w
80	199.148	-2.091	0.019	64.76	0.24	55.51	0.22	0.17	w
81	183.697	10.918	0.079	59.81	0.28	20.45	0.28	0.23	w
82	227.65	54.387	0.038	45.33	0.17	31.73	0.28	0.25	w
83	132.899	39.59	0.041	21.94	0.03	12.23	0.33	0.21	w
84	197.953	10.602	0.031	72.12	0.32	99.54	0.19	0.18	w
85	148.019	6.209	0.062	41.64	0.21	17.88	0.4	0.36	w
86	151.284	44.514	0.026	21.76	0.01	9.94	0.09	0.08	w
87	149.828	52.257	0.04	41.42	0.11	20.9	0.23	0.19	w
88	129.277	41.456	0.029	32.87	0.08	25.36	0.26	0.23	w
89	211.807	45.89	0.04	37.15	0.05	14.83	0.18	0.1	w
90	176.441	47.175	0.054	56.93	0.27	42.66	0.26	0.26	w
91	230.778	37.67	0.065	99.56	1.12	182.24	0.37	0.35	w
92	155.243	6.642	0.033	72.24	0.66	241.78	0.42	0.38	w
93	236.625	32.117	0.032	35.67	0.06	13.17	0.19	0.14	w
94	178.758	49.9	0.059	47.23	0.2	18.99	0.3	0.27	w
95	233.473	45.118	0.072	57.42	0.3	46.64	0.31	0.28	w
96	217.825	7.945	0.027	22.21	0.06	16.58	0.44	0.39	w
97	214.386	8.856	0.037	31.19	0.13	58.02	0.42	0.4	w
98	135.308	6.022	0.076	69.29	0.56	60.34	0.36	0.36	w
99	195.788	54.617	0.028	94.26	0.65	567.47	0.25	0.22	w
100	156.661	37.775	0.051	31.25	0.04	6.42	0.14	0.13	w
101	206.035	45.341	0.038	33.41	0.04	13.39	0.11	0.11	w
102	249.643	31.873	0.064	46.85	0.17	26.79	0.28	0.23	w
103	124.187	27.592	0.04	40.3	0.07	12.53	0.18	0.14	w
104	128.212	30.879	0.066	55.44	0.09	14.32	0.09	0.09	w
105	159.331	43.588	0.025	48.3	0.17	24.45	0.28	0.23	w
106	216.903	41.258	0.009	23.35	0.01	19.28	0.23	0.07	w
107	212.225	10.199	0.067	122.42	1.17	192.69	0.28	0.24	w
108	211.273	11.475	0.067	65.05	0.46	64.63	0.35	0.33	w
109	212.137	11.816	0.019	49.52	0.13	58.11	0.18	0.16	w
110	134.207	35.917	0.076	41.71	0.27	30.19	0.51	0.47	w
111	221.955	47.81	0.037	30.8	0.05	22.88	0.19	0.18	w
112	232.647	33.632	0.065	38.73	0.1	14.78	0.24	0.21	w
113	191.326	42.41	0.053	43.81	0.2	19.85	0.33	0.32	w
114	145.814	35.161	0.05	70.48	0.48	63.55	0.37	0.3	w
115	147.83	36.178	0.052	43.81	0.1	12.75	0.18	0.15	w
116	172.806	40.653	0.045	42.14	0.08	17.39	0.26	0.14	w
117	174.931	42.505	0.07	21.34	0.06	6.43	0.42	0.38	w
118	172.828	42.813	0.045	15.74	0.01	4.16	0.21	0.14	w
119	215.628	11.305	0.016	73.65	0.41	308.29	0.25	0.23	w
120	238.347	26.105	0.069	55.67	0.14	18.51	0.28	0.13	w
121	157.067	38.935	0.055	48.22	0.24	53.78	0.33	0.31	w
122	186.372	47.273	0.025	43.81	0.13	31.38	0.24	0.21	w
123	202.365	55.721	0.043	35.3	0.07	19.55	0.2	0.18	w
124	164.403	44.071	0.034	21.94	0.02	4.68	0.17	0.11	w
125	209.305	12.021	0.021	47.04	0.04	6.14	0.05	0.05	w
126	211.096	11.736	0.02	50.18	0.16	102.7	0.29	0.19	w
127	187.741	10.803	0.049	30.57	0.04	12.19	0.16	0.13	w
128	197.651	39.784	0.047	31.85	0.06	9.21	0.29	0.19	w
129	229.63	32.393	0.061	26.93	0.03	4.46	0.18	0.15	w
130	190.309	12.989	0.047	62.45	0.11	29.38	0.22	0.08	w
131	157.436	40.494	0.044	24.76	0.03	4.18	0.16	0.13	w
132	210.019	58.37	0.026	66.6	0.09	65.88	0.13	0.06	w
133	247.486	39.944	0.059	62.61	0.06	5.69	0.1	0.04	w
134	150.766	12.95	0.036	58.76	0.24	62.72	0.21	0.21	w
135	148.655	6.622	0.041	72.98	0.65	113.74	0.4	0.37	w
136	205.26	13.163	0.056	53.01	0.15	41.25	0.18	0.17	w
137	202.655	14.649	0.067	40.89	0.15	21.57	0.31	0.27	w
138	204.54	14.92	0.059	58.81	0.29	41.0	0.27	0.26	w
139	208.419	56.134	0.035	34.3	0.07	46.78	0.24	0.19	w
140	154.217	39.556	0.064	26.17	0.02	2.75	0.11	0.1	w
141	225.507	9.408	0.046	59.36	0.25	81.22	0.24	0.21	w
142	187.588	7.488	0.067	25.94	0.01	1.26	0.06	0.05	w
143	163.764	42.86	0.059	18.53	0.0	0.84	0.28	0.04	k
144	214.977	51.895	0.029	31.95	0.03	8.43	0.13	0.09	w
145	346.954	0.941	0.042	65.73	0.22	20.31	0.17	0.16	w
146	170.756	47.052	0.025	56.3	0.2	62.76	0.22	0.19	w
147	227.507	10.805	0.047	19.79	0.05	15.29	0.46	0.42	w
148	208.949	14.422	0.052	44.53	0.22	41.1	0.4	0.34	w
149	136.707	26.275	0.021	47.36	0.23	106.29	0.32	0.31	w
150	222.778	37.495	0.032	60.17	0.27	64.95	0.25	0.22	w
151	223.662	12.245	0.077	63.78	0.16	13.63	0.3	0.12	w
152	216.097	13.798	0.017	43.03	0.07	161.35	0.24	0.11	w
153	47.029	0.456	0.074	33.95	0.11	15.19	0.34	0.29	w
154	133.705	57.67	0.014	22.21	0.04	31.16	0.24	0.23	w
155	163.022	41.39	0.036	21.34	0.03	6.05	0.2	0.17	w
156	197.296	52.021	0.026	56.74	0.2	252.18	0.22	0.19	w
157	197.053	52.466	0.055	25.71	0.05	8.02	0.26	0.23	w

Table A1. - continued

Index	RA	DEC	z	σ $km\ s^{-1}$	M_{vir} $10^{12}M_{\odot}$	M_{vir}/L_r M_{\odot}/L_{\odot}	\bar{r}_p Mpc	r_h Mpc	flag
158	180.132	38.611	0.037	45.49	0.13	36.69	0.28	0.19	w
159	236.64	41.918	0.024	7.48	0.0	4.03	0.31	0.26	w
160	181.533	37.326	0.044	17.71	0.03	3.59	0.28	0.25	w
161	147.358	26.638	0.052	44.53	0.08	20.71	0.15	0.12	w
162	230.579	21.073	0.05	54.13	0.07	22.62	0.08	0.08	w
163	198.864	29.074	0.035	37.95	0.07	14.98	0.27	0.14	w
164	241.584	39.244	0.039	61.59	0.27	161.46	0.22	0.22	w
165	225.229	8.582	0.056	27.8	0.03	2.93	0.12	0.11	w
166	242.068	36.093	0.043	77.42	0.61	69.3	0.34	0.31	w
167	244.578	34.111	0.047	66.0	0.35	61.09	0.35	0.24	w
168	231.523	9.204	0.006	35.42	0.07	810.22	0.23	0.18	w
169	233.449	10.78	0.045	20.04	0.06	17.13	0.46	0.43	w
170	135.198	29.99	0.054	57.42	0.33	84.66	0.35	0.3	w
171	200.91	31.127	0.058	36.74	0.07	17.09	0.17	0.16	w
172	168.201	31.813	0.075	84.66	0.21	34.22	0.11	0.09	w
173	179.952	29.641	0.029	64.9	0.26	221.97	0.32	0.19	w
174	143.277	33.138	0.05	60.37	0.16	44.89	0.17	0.14	w
175	239.097	26.158	0.064	45.73	0.11	20.73	0.16	0.16	w
176	322.365	0.033	0.052	19.43	0.01	2.64	0.1	0.1	w
177	148.978	27.457	0.056	64.5	0.19	27.59	0.25	0.14	w
178	123.265	24.567	0.02	35.67	0.01	15.67	0.06	0.03	k
179	201.143	43.752	0.047	42.84	0.08	8.15	0.23	0.13	w
180	225.434	27.281	0.056	54.31	0.23	50.3	0.27	0.24	w
181	217.671	16.054	0.048	59.27	0.4	83.81	0.38	0.34	w
182	212.874	16.755	0.027	64.87	0.57	277.89	0.47	0.41	w
183	218.644	14.097	0.07	56.74	0.16	19.97	0.27	0.15	w
184	155.957	20.985	0.066	12.07	0.01	1.75	0.35	0.3	w
185	154.049	22.26	0.065	60.47	0.17	23.48	0.15	0.14	w
186	165.715	36.783	0.025	49.28	0.15	43.22	0.22	0.19	w
187	208.955	35.151	0.035	43.12	0.12	46.73	0.3	0.19	w
188	166.148	36.654	0.021	18.53	0.01	8.73	0.14	0.06	w
189	169.341	25.066	0.07	21.1	0.04	4.77	0.31	0.3	w
190	137.867	64.475	0.018	37.07	0.04	29.25	0.17	0.08	w
191	213.171	30.855	0.014	45.29	0.05	53.08	0.07	0.07	w
192	237.5	24.802	0.024	70.66	0.19	56.2	0.17	0.11	w
193	140.155	26.538	0.049	57.84	0.15	42.46	0.14	0.14	w
194	217.968	54.722	0.043	69.08	0.43	108.72	0.29	0.27	w
195	219.138	20.516	0.068	45.16	0.11	14.98	0.29	0.16	w
196	122.262	50.179	0.017	50.58	0.05	128.31	0.09	0.06	w
197	122.56	51.873	0.061	6.16	0.0	0.14	0.08	0.08	w
198	162.714	17.83	0.066	19.01	0.03	1.95	0.27	0.23	w
199	161.602	18.531	0.049	28.23	0.06	14.35	0.26	0.23	w
200	200.035	30.45	0.048	43.26	0.02	3.28	0.13	0.04	k
201	151.379	15.373	0.052	90.74	0.06	9.73	0.16	0.02	k
202	238.768	45.486	0.028	32.6	0.07	22.08	0.21	0.2	w
203	205.289	12.772	0.047	31.95	0.08	13.63	0.31	0.23	w
204	195.719	7.681	0.07	58.76	0.23	26.94	0.3	0.2	w
205	244.44	6.065	0.038	69.97	0.2	60.12	0.14	0.13	w
206	238.247	8.016	0.041	27.84	0.05	13.04	0.22	0.21	w
207	193.562	9.442	0.045	58.15	0.09	13.69	0.09	0.08	w
208	194.728	9.301	0.054	14.75	0.01	1.19	0.19	0.13	w
209	222.111	34.998	0.029	49.52	0.34	51.11	0.46	0.42	w
210	222.42	35.69	0.029	30.99	0.03	9.63	0.12	0.11	w
211	226.85	34.076	0.044	11.04	0.01	3.07	0.25	0.2	w
212	205.825	20.314	0.05	11.22	0.0	0.84	0.25	0.09	w
213	157.961	20.926	0.042	35.67	0.1	29.98	0.26	0.24	w
214	185.17	19.107	0.045	101.61	1.18	116.97	0.41	0.35	w
215	131.428	19.726	0.055	40.89	0.09	11.91	0.3	0.16	w
216	133.67	20.584	0.013	61.99	0.15	159.06	0.12	0.12	w
217	133.51	17.343	0.067	31.57	0.04	5.47	0.12	0.12	w
218	134.144	16.809	0.052	38.1	0.09	11.64	0.21	0.18	w
219	210.289	21.238	0.028	30.99	0.02	9.4	0.19	0.05	w
220	188.095	16.31	0.057	8.48	0.0	0.52	0.19	0.17	w
221	181.669	16.477	0.062	79.58	0.12	20.61	0.07	0.06	w
222	166.517	14.036	0.066	10.67	0.01	0.53	0.16	0.15	w
223	166.711	14.457	0.052	75.54	0.27	46.95	0.16	0.14	w
224	143.69	13.816	0.026	43.03	0.12	141.76	0.26	0.2	w
225	142.253	12.504	0.052	29.2	0.12	19.22	0.5	0.44	w
226	122.272	55.442	0.031	9.89	0.01	4.34	0.31	0.31	w
227	194.629	24.974	0.076	66.63	0.37	29.15	0.34	0.25	w
228	138.93	15.22	0.03	31.25	0.06	19.24	0.21	0.18	w
229	194.542	24.349	0.023	28.69	0.06	64.35	0.25	0.24	w
230	333.072	0.268	0.045	45.49	0.16	49.91	0.25	0.23	w
231	120.62	20.514	0.029	40.69	0.18	113.04	0.35	0.34	w
232	199.703	12.397	0.037	17.65	0.01	4.89	0.12	0.12	w
233	213.152	-1.036	0.054	30.61	0.05	10.65	0.2	0.16	w
234	125.412	8.346	0.052	48.22	0.1	20.21	0.2	0.13	w
235	141.748	20.884	0.051	58.76	0.44	72.27	0.45	0.39	w
236	214.13	57.81	0.01	37.39	0.03	42.66	0.13	0.07	w
237	147.465	10.432	0.029	34.99	0.04	18.74	0.24	0.1	w

Table A1. - continued

Index	RA	DEC	z	σ $km\ s^{-1}$	M_{vir} $10^{12}M_{\odot}$	M_{vir}/L_r M_{\odot}/L_{\odot}	\bar{r}_p Mpc	r_h Mpc	flag
238	191.639	43.743	0.041	19.12	0.03	10.44	0.3	0.26	w
239	187.382	33.427	0.031	53.35	0.13	111.86	0.15	0.14	w
240	31.683	13.372	0.061	67.67	0.36	86.8	0.26	0.24	w
241	235.652	21.129	0.047	19.94	0.06	15.05	0.49	0.44	w
242	236.745	17.884	0.011	36.96	0.02	19.6	0.06	0.04	w
243	217.107	17.924	0.019	19.79	0.01	4.44	0.28	0.12	w
244	158.708	17.451	0.056	91.82	0.52	72.93	0.27	0.19	w
245	242.707	21.051	0.038	89.03	0.13	39.42	0.25	0.05	w
246	219.967	42.742	0.008	35.67	0.04	55.35	0.19	0.09	w
247	197.297	46.316	0.035	65.82	0.13	25.17	0.14	0.09	w
248	201.996	45.759	0.061	52.63	0.24	29.6	0.3	0.26	w
249	201.44	46.162	0.036	25.79	0.04	14.48	0.18	0.17	w
250	215.921	47.372	0.073	39.34	0.11	14.02	0.22	0.21	w
251	135.03	60.083	0.039	43.54	0.06	17.61	0.14	0.09	w
252	323.752	-0.511	0.03	47.21	0.08	37.76	0.32	0.1	w
253	245.924	24.172	0.043	60.07	0.4	73.32	0.4	0.34	w
254	156.546	32.099	0.037	123.63	0.67	77.02	0.24	0.13	w
255	162.117	38.294	0.033	15.55	0.01	4.05	0.16	0.15	w
256	171.133	39.787	0.061	46.72	0.16	26.04	0.33	0.23	w
257	165.93	29.242	0.066	40.07	0.1	15.4	0.23	0.18	w
258	166.433	35.884	0.068	75.41	0.49	92.75	0.34	0.26	w
259	145.456	25.064	0.051	17.13	0.01	1.54	0.22	0.12	w
260	185.047	27.68	0.08	59.07	0.18	12.74	0.21	0.16	w
261	247.377	13.083	0.033	49.99	0.08	34.67	0.13	0.1	w
262	245.762	26.538	0.04	51.01	0.06	27.01	0.08	0.08	w
263	229.252	15.566	0.048	25.71	0.01	1.36	0.08	0.06	w
264	199.061	41.494	0.021	31.82	0.02	7.29	0.05	0.05	w
265	223.593	27.701	0.034	25.9	0.05	17.4	0.34	0.21	w
266	188.546	21.542	0.045	22.74	0.01	2.69	0.13	0.04	w
267	220.738	17.637	0.056	40.69	0.11	23.26	0.23	0.21	w
268	143.318	23.135	0.026	33.05	0.06	33.82	0.27	0.18	w
269	147.104	22.363	0.034	21.94	0.02	8.91	0.2	0.15	w
270	113.634	41.215	0.043	99.2	0.11	33.67	0.04	0.03	k
271	162.004	28.246	0.021	40.39	0.08	21.98	0.18	0.15	w
272	222.889	45.438	0.037	66.24	0.12	48.1	0.22	0.09	w
273	175.759	23.944	0.023	61.99	0.2	76.86	0.17	0.16	w
274	143.518	17.832	0.027	41.64	0.08	27.9	0.21	0.15	w
275	208.292	17.332	0.026	26.85	0.04	11.85	0.32	0.18	w
276	210.442	18.808	0.028	58.05	0.12	85.61	0.12	0.11	w
277	178.224	21.835	0.038	83.16	0.2	56.47	0.11	0.09	w
278	220.809	16.488	0.037	59.57	0.11	21.82	0.11	0.09	w
279	229.829	13.126	0.034	51.89	0.31	150.8	0.37	0.35	w
280	128.417	9.964	0.031	26.17	0.02	5.09	0.1	0.09	w
281	130.646	10.585	0.007	21.2	0.03	219.44	0.3	0.17	w
282	201.334	18.453	0.022	35.56	0.08	24.98	0.36	0.19	w
283	228.95	18.379	0.038	46.21	0.09	18.58	0.16	0.13	w
284	250.806	25.34	0.055	64.59	0.23	39.97	0.19	0.17	w
285	135.797	10.152	0.03	31.19	0.04	13.6	0.21	0.12	w
286	194.695	32.192	0.052	96.71	0.23	31.8	0.08	0.08	w
287	208.915	20.744	0.075	39.57	0.13	13.94	0.36	0.25	w
288	208.53	21.975	0.063	47.21	0.16	10.72	0.22	0.22	w
289	234.764	13.637	0.05	65.18	0.41	60.82	0.36	0.3	w
290	230.4	14.384	0.025	45.16	0.13	152.92	0.21	0.19	w
291	38.702	-7.684	0.022	44.06	0.04	13.5	0.27	0.07	w
292	128.168	19.511	0.021	24.64	0.06	85.41	0.32	0.29	w
293	126.569	17.362	0.066	30.21	0.07	5.76	0.24	0.23	w
294	192.894	5.864	0.049	84.45	0.33	56.25	0.17	0.14	w
295	162.974	10.099	0.026	50.54	0.06	34.61	0.08	0.07	w
296	155.252	27.238	0.038	47.78	0.15	48.1	0.24	0.19	w
297	126.523	13.009	0.044	27.07	0.02	5.32	0.26	0.09	w
298	177.897	17.931	0.038	36.83	0.06	17.54	0.13	0.12	w
299	139.151	25.303	0.043	19.01	0.01	2.94	0.17	0.1	w
300	241.399	16.526	0.016	14.13	0.03	69.25	0.54	0.5	w
301	209.329	15.458	0.018	96.71	0.2	50.52	0.21	0.06	w
302	138.357	17.124	0.056	12.95	0.01	1.86	0.24	0.12	w
303	49.846	0.823	0.034	49.14	0.03	16.08	0.3	0.04	k
304	129.472	12.781	0.03	33.41	0.04	13.4	0.21	0.1	w
305	226.674	23.642	0.016	10.19	0.01	3.04	0.27	0.24	w
306	202.446	6.465	0.054	56.74	0.37	69.09	0.39	0.35	w
307	165.874	16.37	0.047	36.83	0.12	13.5	0.28	0.26	w
308	127.046	10.541	0.031	54.31	0.22	97.78	0.26	0.23	w
309	179.361	7.461	0.032	26.4	0.1	21.91	0.48	0.43	w
310	130.642	11.699	0.077	51.71	0.11	6.89	0.14	0.12	w
311	219.595	18.111	0.03	17.13	0.02	6.65	0.31	0.18	w
312	246.783	9.096	0.046	87.03	0.8	262.79	0.34	0.32	w
313	223.748	18.037	0.02	20.91	0.03	9.08	0.31	0.23	w
314	219.307	19.422	0.03	53.31	0.18	98.43	0.31	0.2	w
315	175.664	24.823	0.021	50.3	0.18	78.2	0.3	0.22	w

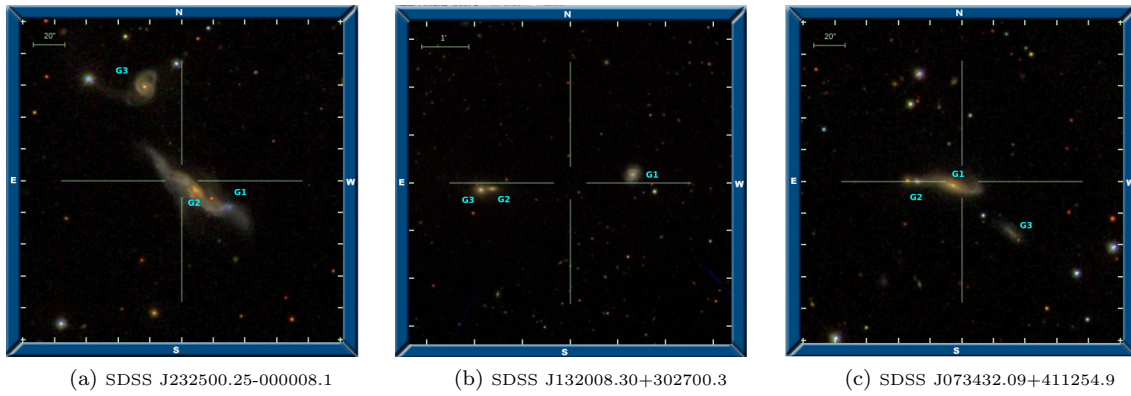


Figure A1. SDSS color images of three compact triplet systems from the selected catalogue of isolated galaxy triplet

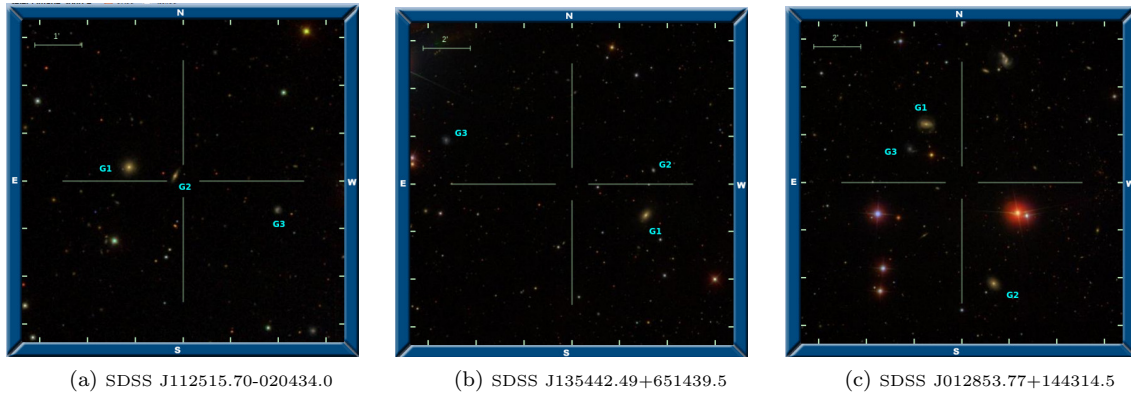


Figure A2. SDSS color images of three wide triplet systems from the selected catalogue of galaxy triplet sample